



HAL
open science

Spin and recombination dynamics of excitons and free electrons in p-type GaAs: Effect of carrier density

Fabian Cadiz, David Lagarde, Pierre Renucci, D. Paget, Thierry Amand, H el ene Carr ere, H. Rowe, S. Arscott

► **To cite this version:**

Fabian Cadiz, David Lagarde, Pierre Renucci, D. Paget, Thierry Amand, et al.. Spin and recombination dynamics of excitons and free electrons in p-type GaAs: Effect of carrier density. *Applied Physics Letters*, 2017, 110 (8), pp.082101. <10.1063/1.4977003>. <hal-02053976>

HAL Id: hal-02053976

<https://insa-toulouse.hal.science/hal-02053976v1>

Submitted on 27 May 2022

HAL is a multi-disciplinary open access archive for the deposit and dissemination of scientific research documents, whether they are published or not. The documents may come from teaching and research institutions in France or abroad, or from public or private research centers.

L'archive ouverte pluridisciplinaire **HAL**, est destin ee au d ep ot et  a la diffusion de documents scientifiques de niveau recherche, publi es ou non,  emanant des  tablissements d'enseignement et de recherche fran ais ou  trangers, des laboratoires publics ou priv es.



HAL Authorization

Spin and recombination dynamics of excitons and free electrons in p-type GaAs: Effect of carrier density

Cite as: Appl. Phys. Lett. **110**, 082101 (2017); <https://doi.org/10.1063/1.4977003>

Submitted: 08 November 2016 • Accepted: 06 February 2017 • Published Online: 21 February 2017

F. Cadiz, D. Lagarde, P. Renucci, et al.



View Online



Export Citation



CrossMark

ARTICLES YOU MAY BE INTERESTED IN

[Ambipolar spin diffusion in p-type GaAs: A case where spin diffuses more than charge](#)

Journal of Applied Physics **122**, 095703 (2017); <https://doi.org/10.1063/1.4985831>

[Electronic analog of the electro-optic modulator](#)

Applied Physics Letters **56**, 665 (1990); <https://doi.org/10.1063/1.102730>

[Band parameters for III-V compound semiconductors and their alloys](#)

Journal of Applied Physics **89**, 5815 (2001); <https://doi.org/10.1063/1.1368156>

Lock-in Amplifiers
up to 600 MHz



Zurich
Instruments



Spin and recombination dynamics of excitons and free electrons in p-type GaAs: Effect of carrier density

F. Cadiz,^{1,2} D. Lagarde,¹ P. Renucci,¹ D. Paget,² T. Amand,¹ H. Carrère,¹ A. C. H. Rowe,² and S. Arscott³

¹Université de Toulouse, INSA-CNRS-UPS, 31077 Toulouse Cedex, France

²Laboratoire de Physique de la Matière Condensée, Ecole Polytechnique, CNRS, Université Paris Saclay, 91128 Palaiseau, France

³Institut d'Electronique, de Microélectronique et de Nanotechnologie (IEMN), CNRS, University of Lille, Avenue Poincaré, Cité Scientifique, 59652 Villeneuve d'Ascq, France

(Received 8 November 2016; accepted 6 February 2017; published online 21 February 2017)

Carrier and spin recombination are investigated in p-type GaAs of acceptor concentration $N_A = 1.5 \times 10^{17} \text{ cm}^{-3}$ using time-resolved photoluminescence spectroscopy at 15 K. At low photocarrier concentration, acceptors are mostly neutral and photoelectrons can either recombine with holes bound to acceptors ($e\text{-}A^0$ line) or form excitons which are mostly trapped on neutral acceptors forming the (A^0X) complex. It is found that the spin relaxation is faster for free electrons that recombine through the $e\text{-}A^0$ transition due to exchange scattering with either trapped or free holes, whereas spin flip processes are less likely to occur once the electron forms with a free hole an exciton bound to a neutral acceptor. An increase in the photocarrier concentration induces a cross-over to a regime where the bimolecular band-to-band (b-b) emission becomes more favorable due to screening of the electron-hole Coulomb interaction and ionization of excitonic complexes and free excitons. Then, the formation of excitons is no longer possible, the carrier recombination lifetime increases and the spin lifetime is found to decrease dramatically with a concentration due to fast spin relaxation with free photoholes. In this high density regime, both the electrons that recombine through the $e\text{-}A^0$ transition and through the b-b transition have the same spin relaxation time. Published by AIP Publishing. [<http://dx.doi.org/10.1063/1.4977003>]

Characterization of charge and spin dynamics in semiconductors is of importance for the designing of devices, such as photovoltaic, microelectronic, and spintronics systems. For p-type GaAs, there have been numerous investigations of the photoluminescence spectrum,^{1–4} as well as of the recombination,^{5–8} spin dynamics,⁹ and spin-polarized transport.^{10,11} Among these investigations, the carrier and spin dynamics of the p-type material of intermediate doping ($\sim 10^{17} \text{ cm}^{-3}$) considered here has been relatively little investigated.^{12,13} However, the electron mobility is anticipated to be spin-dependent in this doping range.¹¹ Moreover, the effect of carrier concentration on this dynamics is still poorly known.^{14,15}

In the present work, we investigate charge and spin dynamics as a function of photocarrier density. These experiments were performed at $T = 15 \text{ K}$ on a $3 \mu\text{m}$ thick GaAs film (Be acceptor concentration $N_A = 1.5 \times 10^{17} \text{ cm}^{-3}$), passivated on both sides by a GaInP layer which confines the photocreated carriers and strongly decreases surface recombination, which we consider to be negligible at low temperature. At 15 K and for this doping level, the acceptors are mostly neutral¹⁶ and there are two main channels for the electrons to recombine radiatively, either with holes bound to acceptor atoms ($e\text{-}A^0$ line) or via exciton formation and trapping on acceptors which results in the luminescence of the exciton bound to the acceptor line (A^0X). These two lines are shown in Fig. 1(a), under a 2 mW, cw σ^+ -circularly polarized excitation at 1.59 eV, focused onto a beam of $100 \mu\text{m}$ diameter. The A^0X line exhibits a small high energy

shoulder at $\sim 1.52 \text{ eV}$ corresponding to free exciton recombination (X), identified via the temperature-dependent reflectivity and photoluminescence excitation spectroscopy (see [supplementary material](#)). The identification of these lines is in agreement with a previous report.¹ Remarkably, the steady-state circular polarization is different for the two transitions, being lower for the $e\text{-}A^0$ line (4%) than for the A^0X line (7%).

We use time-resolved photoluminescence (TRPL) in order to determine the charge and spin lifetimes as a function of excitation power with a spectral selectivity to A^0X or to $e\text{-}A^0$ luminescence. As described in Refs. 17 and 18, the excitation source was a circularly polarized mode-locked Ti:Sa laser (1.5 ps pulse width, wavelength 780 nm) and the emitted light was dispersed by a spectrometer (resolution 0.12 nm) and detected by a ps streak camera. Here, a repetition frequency of 4 MHz was employed, thanks to the inclusion of a pulse picker. The time-averaged power was adjusted between 2.5 and 5000 μW , and since the diameter of the excitation spot ($100 \mu\text{m}$) was much larger than the diffusion length, lateral diffusion is negligible. An averaged power of 1 μW corresponds, therefore, to a pump fluence of $3.2 \times 10^{-3} \mu\text{J}/\text{cm}^2$ or $1.25 \times 10^{10} \text{ photons}/\text{cm}^2$.

Fig. 1(b) shows the PL spectra at 15 K for different time-delays after the excitation pulse (each curve has been normalized in magnitude). The photoelectron concentration n_0 immediately after the pulse varies between $2.4 \times 10^{14} \text{ cm}^{-3}$ and $5 \times 10^{17} \text{ cm}^{-3}$ for pump fluences between $8 \times 10^{-3} \mu\text{J}/\text{cm}^2$ and $16 \mu\text{J}/\text{cm}^2$, respectively. A key information obtained from the high energy part of

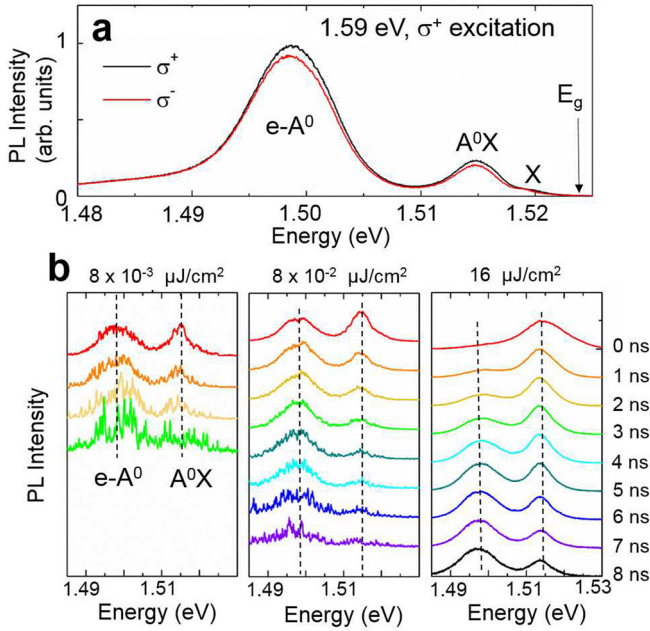


FIG. 1. (a) Polarization-resolved photoluminescence spectrum under cw circularly polarized excitation, revealing that the two main radiative recombination channels correspond to the $e\text{-}A^0$ and to the A^0X transitions. The vertical arrow indicates the position of the bandgap. (b) Transient luminescence spectra at different time delays after the excitation pulse, for a pump fluence of $8 \times 10^{-3} \mu\text{J}/\text{cm}^2$ (left panel, where spectra after 3 ns have been omitted because of their weak signal-to-noise), $8 \times 10^{-2} \mu\text{J}/\text{cm}^2$ (center panel), and $16 \mu\text{J}/\text{cm}^2$ (right panel).

these spectra at high densities is the temperature T_e of the photoelectron gas and its possible time-dependence. It has been found that while heating of the electron gas is significant at high power and during the laser pulse, T_e rapidly decreases to a steady value of 50 K in a time scale of hundreds of ps (see Fig. S5 of the [supplementary material](#)). The hole concentration in the dark p_0 is estimated using

standard semiconductor statistics¹⁹ to $\sim 10^{16} \text{cm}^{-3}$ at 50 K, so that the majority of acceptors are neutral, $N_A^0 \approx 0.9 N_A = 1.35 \times 10^{17} \text{cm}^{-3}$.

For a very weak pump fluence (left panel), the $e\text{-}A^0$ line is dominant at all delays after the pulse. The center panel shows the spectra for a fluence of $8 \times 10^{-2} \mu\text{J}/\text{cm}^2$, and shows that the two lines have similar intensities immediately after the pulse, while the $e\text{-}A^0$ line again becomes dominant after a delay of about 1 ns. At the highest fluence of $16 \mu\text{J}/\text{cm}^2$ (right panel), the exciton formation is completely inhibited due to screening^{20,21} and the spectrum exhibits mostly band to band (b-b) emission which recombines faster than the $e\text{-}A^0$ line due to its bi-molecular nature. Note that screening produces a blueshift of the A^0X line towards the X emission, whereas the b-b emission energy redshifts due to bandgap renormalization. In addition to a spectral broadening at high fluence, this is responsible for the negligible overall shift of the higher energy line of the spectrum.²¹ This type of crossover, identified as a Mott transition between an excitonic regime towards an electron-hole plasma regime due to screening of the electron-hole interaction,^{20,22} has never been reported so far in the p-type material. An independent confirmation of exciton screening at high densities can be obtained by analyzing the energy-resolved circular polarization around the A^0X /b-b line as a function of excitation power (see Fig. S3 of the [supplementary material](#)).

The intensity transients integrated over each spectral line are summarized in panel (a) of Fig. 2; the degree of circular polarization of each line, defined as $\mathcal{P} = (I^{\sigma^+} - I^{\sigma^-}) / (I^{\sigma^+} + I^{\sigma^-})$ where I^{σ^\pm} represents the σ^\pm -polarized component of the luminescence, is also shown in panel (b) of Fig. 2. These transients directly yield the photoelectron recombination and spin relaxation time.

We first discuss the lifetime τ_{PL} of both lines as a function of the pump fluence. At low densities, both lines are characterized by a similar decay time of $\tau_{A^0X} = 0.7 \pm 0.05$ ns

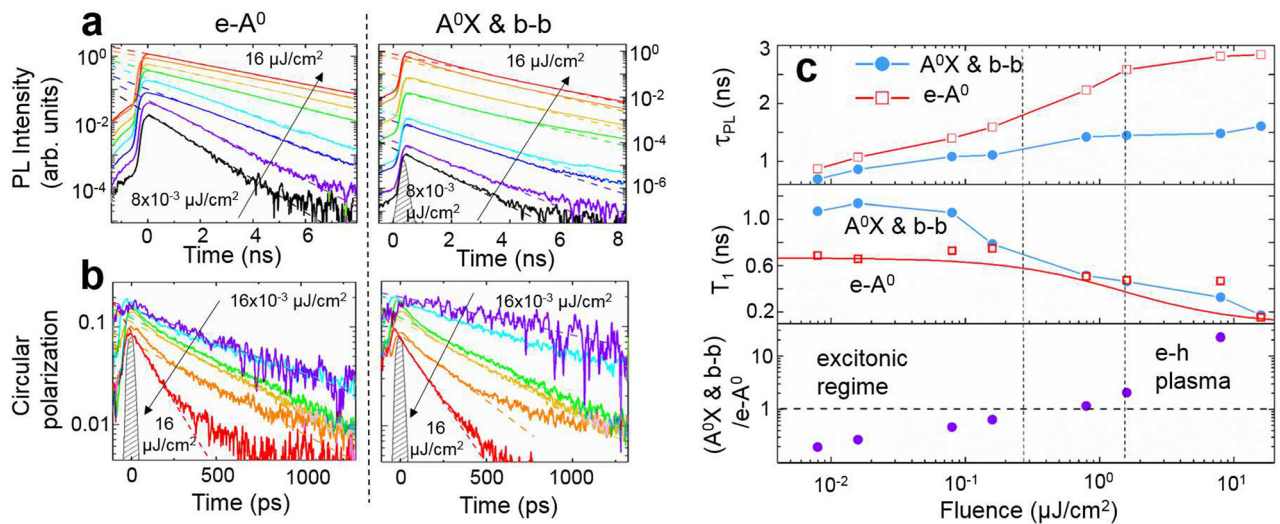


FIG. 2. (a) Normalized intensity transients for the $e\text{-}A^0$ line (left panel) and for the A^0X line which merges with b-b recombination at high fluence (right panel). The pump fluence for each transient varies between $8 \times 10^{-3} \mu\text{J}/\text{cm}^2$ and $16 \mu\text{J}/\text{cm}^2$. The curves have been shifted for clarity. Also shown is the response of the setup (filled curve in the right panel). (b) Decay transients of the luminescence degree of circular polarization for the $e\text{-}A^0$ line (left panel) and for the A^0X line (right panel), for a pump fluence between $16 \times 10^{-3} \mu\text{J}/\text{cm}^2$ and $16 \mu\text{J}/\text{cm}^2$. (c) The top panel shows the fluence dependence of the PL decay times for the two lines, and the middle panel shows the spin relaxation time found for the two lines, as a function of pump fluence. The bottom panel shows the ratio of the spectrally integrated intensity for the higher energy line ($A^0X + \text{b-b}$) to the $e\text{-}A^0$ line at $t = 0$, and reveals the existence of a crossover at a fluence of about $3 \times 10^{-1} \mu\text{J}/\text{cm}^2$. The symbols represent the experimental data, and the solid lines are a guide to the eye, except from the lower curve of the middle panel which is a fit obtained using Eq. (3).

and $\tau_{e-A^0} = 0.9 \pm 0.05$ ns for A^0X and $e-A^0$, respectively. In contrast, at the highest fluence, the $e-A^0$ line decays with $\tau_{e-A^0} = 2.8$ ns whereas the b-b recombination has a lifetime of almost half of that of $e-A^0$ line, $\tau_{b-b} = 1.6$ ns. The extracted lifetimes are shown in the top panel of Fig. 2(c), where it can be seen that the recombination time for both lines is a monotonic increasing function of the pump fluence. The observed behaviour has a simple interpretation. At low densities (excitonic regime), since at short time-delays both $e-A^0$ and A^0X lines are present in the spectrum, we assume that during the laser pulse and the subsequent energy relaxation and thermalization, two populations are created, consisting of free electron-hole pairs and of excitons bound to acceptors, respectively. We assume that once the process of thermalization is over, both populations evolve independently as a function of time. For the $e-A^0$ emission, the luminescence intensity is proportional to $K_0 N_A^0 n$ where n is the photoelectron concentration, N_A^0 is the concentration of neutral acceptors, and K_0 is the bimolecular recombination coefficient between a free electron and a hole bound to acceptor. We assume for simplicity that n is homogeneous as a function of depth, and this concentration is the solution of $\partial n / \partial t = -K_0 N_A^0 n - n / \tau_{nr}$ for $t > 0$ with initial condition $n(t=0) = n_0$, where τ_{nr} is a non-radiative lifetime, which we introduce in order to account for the relatively short lifetime of the $e-A^0$ emission. Indeed, using Ref. 23 we calculate an acceptor recombination time of $1/(K_0 N_A^0) = 15$ ns, which is more than one order of magnitude larger than the measured lifetime of the $e-A^0$ line. We conclude that the photoelectron lifetime is limited by nonradiative recombination, for example, via free exciton formation or capture of free carriers by deep level centers.^{24,25} Note that the fact that the intensity decay transients of Fig. 2(a) are mono-exponential at low pump fluence suggests that in this regime the main recombination mechanism is given by trapping at deep level centers. Since the A^0X line decays with a similar lifetime, we conclude that the lifetime of excitons bound to acceptors is probably also limited by non-radiative recombination, for example, via free exciton formation at a rate similar to $1/\tau_{nr}$. Indeed, excitons bound to acceptors have a binding energy of ~ 2 meV $< k_B T_e$ with respect to the free exciton state, so that coupling with free excitons should be efficient. We assume that free-excitons have a very short non-radiative lifetime (for example, via formation and escape of exciton-polaritons,²⁶⁻²⁹ or via trapping at deep centers, so that they cannot dissociate or get trapped again at acceptor sites.

On the other hand, at high fluence, exciton formation is inhibited, recombination at deep level centers saturates, and the electron lifetime increases with concentration when passing from A^0X recombination to b-b recombination. It is seen that the A^0X line eventually merges with the band-to-band recombination emission whose intensity is proportional to $n K_{bb} [n + p_0]$, where the bimolecular coefficient K_{bb} with free holes has been already calculated³⁰ and where one assumes that the photohole and photoelectron concentrations are equal because of charge neutrality.³¹ In this electron-hole plasma regime, and neglecting non-radiative recombination, the photoelectron concentration evolves according to $\partial n / \partial t = -K_0 N_A^0 n - K_{bb} [n + p_0] n$. This equation has an

analytical solution, and the intensity of the luminescence of the two lines is given by

$$I(e-A^0)(t) = AK_0 N_A^0 n_0 \frac{e^{-t/\tau^*}}{1 + n_0 K_{bb} \tau^* [1 - e^{-t/\tau^*}]}, \quad (1)$$

$$I(b-b)(t) = \frac{K_{bb} p_0}{K_0 N_A^0} I(e-A^0)(t) + \frac{AK_{bb} n_0^2 e^{-2t/\tau^*}}{\{1 + n_0 K_{bb} \tau^* [1 - e^{-t/\tau^*}]\}^2}, \quad (2)$$

where $1/\tau^* = K_0 N_A^0 + K_{bb} p_0$. While increasing the photocarrier density, the second term of Eq. (2) becomes progressively dominant so that the characteristic decay time of the b-b line, $\tau_{PL}^{b-b} \approx 1/(K_{bb} n_0)$, should be one half that of the $e-A^0$ one, as indeed observed in our experiments. It is also expected that the departure from a mono-exponential behavior should be stronger for the b-b line than for the eA_0 one, which is indeed the case at short delays and high fluence (see the right panel of Fig. 2(a)). The bimolecular recombination coefficient K_{bb} at a carrier temperature of $T_e = 50$ K is $K_{bb} = 4.27 \times 10^{-9}$ cm³/s.³⁰ Since $\tau_{PL}^{b-b} \approx 1.6$ ns at the maximum fluence used, we estimate a characteristic photocarrier concentration of $\approx 1/(\tau_{PL}^{b-b} K_{bb}) = 1.46 \times 10^{17}$ cm⁻³ at $t=0$ when exciting at 16 μ J/cm².

We now focus on the spin dynamics. Figure 2(b) shows the transients of the luminescence degree of circular polarization \mathcal{P} for selected pump fluences. Note that the polarization immediately after the pulse, of the order of 15%, is smaller than the initial polarization of 25% expected for GaAs. This reveals losses of polarization during fast energy relaxation and thermalization of the carriers. The polarization transients are essentially exponential and enable us to determine a well-defined spin relaxation time T_1 for both lines, as summarized in the middle panel of Fig. 2(c). T_1 is found to decrease significantly with the fluence in the range explored (from $T_1 \approx 1$ ns at low fluence for the A^0X line to $T_1 \approx 150$ ps for the b-b line at high densities). Interestingly, T_1 is lower for the $e-A^0$ line than for the A^0X line at low densities, whereas the same spin relaxation time is found at high fluence for both lines. We can interpret these findings as spin relaxation induced by scattering between photoelectrons and holes (Bir-Aronov-Pikus mechanism),³² which has been shown to be the dominant spin relaxation mechanism at low temperatures for the p-doping level used here.^{9,33,34} This scenario is further supported by temperature-dependent measurements, in which the spin polarization is shown to decrease dramatically as the concentration of free holes increases with temperature (see Figure S6 of the [supplementary material](#)). The free electron spin relaxation time is given by⁹

$$\frac{1}{T_1} = \frac{1}{T_1^0} \left[|\psi(0)|^4 \frac{N_A^- + p}{N_A + p} + \frac{5}{3} \left(1 - \frac{N_A^- + p}{N_A + p} \right) \right], \quad (3)$$

where $1/T_1^0 = N_A a_B^3 \frac{2v_e}{\tau_0 v_B}$, $a_B = 1.13 \times 10^{-8}$ m is the exciton Bohr radius, $v_B = \hbar/(\mu_X a_B) = 1.7 \times 10^5$ m/s is the exciton Bohr velocity with $\mu_X \approx m_e^*$ the exciton reduced mass and m_e^* the electron's effective mass in the conduction band, $v_e = \sqrt{3k_B T_e / m_e^*}$ is the thermal velocity of electrons, τ_0

$= \hbar E_B / \Delta^2 = 1.1$ ns can be estimated from the exchange splitting $\Delta \sim 0.05$ meV of the exciton ground state^{35,36} and from the exciton binding energy $E_B = 4.2$ meV,³⁷ p represents the density of photoholes, N_A^- is the density of ionized acceptors, and $|\psi(0)|^2$ is the Sommerfeld factor, estimated to be $|\psi(0)|^2 \approx 2\pi$ for $T_e = 50$ K.^{38,39} We estimate $T_1^0 = 3.63$ ns. At low concentrations, $p \ll N_A^- \approx 0.1N_A$ and therefore $T_1 \approx T_1^0 / (39.47 \times 0.1 + 5/3 \times 0.9) = 667$ ps, which agrees remarkably well with the measured spin relaxation time of 690 ps for the e-A⁰ line at low fluence. Interestingly, the spin relaxation time for the A⁰X is almost twice as long, because in the A⁰X complex (one electron and two holes on AA⁻) the total electron-hole exchange interaction vanishes since the stable state of A⁰X involves a hole singlet of the form $\frac{1}{\sqrt{2}}(\uparrow\downarrow - \downarrow\uparrow)$. The observed spin relaxation time of about 1.1 ns for a trapped electron in the A⁰X complex may be limited by the hyperfine interaction⁴⁰ with the atomic nuclei (see [supplementary material](#)) or by exchange interaction with free holes or free electrons. None of the latter two relaxation mechanisms should affect the spin of free electrons.

At high densities, the measured spin lifetime is the same for both lines, as expected since in this regime excitons are no longer stable. Using the above estimated value for the characteristic photocarrier concentration (1.46×10^{17} cm⁻³ $\approx N_A$) at the highest fluence, we have $p \approx n \gg N_A^-$ and therefore $T_1 \approx T_1^0 / (39.47 \times 0.63 + 5/3 \times 0.36) = 140$ ps, which agrees well with the measured value of $T_1 \sim 150$ ps considering that screening has been neglected in Eq. (3). The solid red curve shown in the middle panel of Fig. 2(c) is the spin lifetime given by Eq. (3) as a function of excitation power, assuming that the photocarrier concentration depends linearly on fluence. This equation reproduces well the observed decrease of the spin lifetime for the e-A⁰ line as the concentration of free carriers increases.

The results obtained for the present sample are quite different from those obtained for a larger acceptor concentration, in the 10^{18} cm⁻³ range, which shows little dependence of the spin relaxation time and carrier lifetime as a function of pump fluence,¹⁸ probably due to more efficient screening of the electron-hole interaction and almost full ionization of acceptors.^{41,42} Also shown in the bottom panel of Fig. 2(c) is the ratio between the spectrally integrated higher energy line (mixture of A⁰X and b-b) to the e-A⁰ line immediately after the pulse. For sufficiently large densities, the photoexcited carrier concentration is higher than the concentration of neutral acceptors, and the ratio becomes greater than 1. The dashed line to the left represents the pump fluence at which the photogenerated density at $t=0$ equals the theoretical Mott density in GaAs at $T=0$ K ($n_c = 2.8 \times 10^{16}$ cm⁻³),²¹ whereas the dashed line to the right corresponds to the experimental value of the Mott density in undoped GaAs ($n_c = 1.2 - 1.8 \times 10^{17}$ cm⁻³).²⁰ Independent investigations have shown that screening of the exciton gas start to occur above $n = 1.6 \times 10^{16}$ cm⁻³.⁴³ This screening, together with a saturation of deep level centers, explains the progressive increase of the recombination time and the fact that the two lines are characterized by the same spin relaxation time for an excitation power larger than 2×10^{-1} μ J/cm².

In summary, a systematic study of the carrier and spin recombination dynamics on moderately doped p-type GaAs has been performed at 15 K. It has been shown that at low densities, electrons can form exciton complexes (A⁰X) or recombine with holes bound to neutral acceptors, so that a full thermodynamical equilibrium is not achieved between free and trapped electrons in A⁰X. The lifetime of free and trapped (on A⁰X) electrons is limited by non-radiative recombination channels (the determination of the exact nature of these channels is beyond the scope of this paper and would require further investigations), and the spin lifetime is larger in exciton complexes than for free electrons since the electron-hole exchange interaction is suppressed within the A⁰X complex when excitons are trapped on neutral acceptors. In this density range, the free electron's spin lifetime is limited by exchange scattering between electrons and trapped holes. Increasing the carrier concentration causes screening of the electron-hole Coulomb interaction and eventually excitons are no longer stable. As a consequence, the recombination lifetime increases with concentration and the spin lifetime of free electrons decreases by almost one order of magnitude due to accelerated spin relaxation when free photoholes are added to the system.

See [supplementary material](#) for the reflectivity, photoluminescence excitation spectroscopy, and temperature-dependent measurements.

F.C. and P.R. thank the Grant NEXT No. ANR-10-LABX-0037 in the framework of the Programme des Investissements d'Avenir.

- ¹G. B. Scott, G. Duggan, P. Dawson, and G. Weimann, *J. Appl. Phys.* **52**, 6888 (1981).
- ²R. Dingle, C. Weisbuch, H. L. Stormer, H. Morkoc, and A. Y. Cho, *Appl. Phys. Lett.* **40**, 507 (1982).
- ³H. Chen, M. Feng, P. Chen, K. Lin, and J. Wu, *Jpn. J. Appl. Phys.* **33**, 1920 (1994).
- ⁴M. S. Feng, C. S. A. Fang, and H. D. Chen, *Mater. Chem. Phys.* **42**, 143 (1995).
- ⁵R. J. Nelson and R. G. Sobers, *J. Appl. Phys.* **49**, 6103 (1978).
- ⁶R. J. Seymour and R. R. Alfano, *Appl. Phys. Lett.* **37**, 231 (1980).
- ⁷H. Horinaka, D. Ono, W. Zhen, K. Wada, Y. Cho, Y. Hayashi, T. Nakanishi, S. Okumi, H. Aoyagi, T. Saka *et al.*, *Jpn. J. Appl. Phys.* **34**, 6444 (1995).
- ⁸R. Shinohara, K. Yamaguchi, H. Hirota, Y. Suzuki, T. Manago, H. Akinaga, T. Kuroda, and F. Minami, *Jpn. J. Appl. Phys.* **39**, 7093 (2000).
- ⁹K. Zerrouati, F. Fabre, G. Bacquet, J. Bandet, J. Frandon, G. Lampel, and D. Paget, *Phys. Rev. B* **37**, 1334 (1988).
- ¹⁰F. Cadiz, D. Paget, and A. C. H. Rowe, *Phys. Rev. Lett.* **111**, 246601 (2013).
- ¹¹F. Cadiz, D. Paget, A. C. H. Rowe, T. Amand, P. Barate, and S. Arscott, *Phys. Rev. B* **91**, 165203 (2015).
- ¹²N. Asaka, R. Harasawa, S. Lu, P. Dai, and A. Tackeuchi, *Appl. Phys. Lett.* **104**, 112404 (2014).
- ¹³C. Zhao, T. Yan, H. Ni, Z. Niu, and X. Zhang, *Appl. Phys. Lett.* **102**, 012406 (2013).
- ¹⁴A. Amo, L. Vina, P. Lugli, C. Tejedor, A. I. Toropov, and K. S. Zhuravlev, *Phys. Rev. B* **75**, 085202 (2007).
- ¹⁵H. Zhao, M. Mower, and G. Vignale, *Phys. Rev. B* **79**, 115321 (2009).
- ¹⁶S. Kim, C. Son, S. Chung, Y. Park, E. Kim, and S. Min, *Thin Solid Films* **310**, 63 (1997).
- ¹⁷T. T. Zhang, P. Barate, C. T. Nguyen, A. Balloch, T. Amand, P. Renucci, H. Carrere, B. Urbaszek, and X. Marie, *Phys. Rev. B* **87**, 041201(R) (2013).
- ¹⁸F. Cadiz, P. Barate, D. Paget, D. Grebenkov, J. P. Korb, A. C. H. Rowe, T. Amand, S. Arscott, and E. Peytavit, *J. Appl. Phys.* **116**, 023711 (2014).

- ¹⁹R. A. Smith, *Semiconductors* (Cambridge University Press, Cambridge, 1978).
- ²⁰A. Amo, M. D. Martin, L. Vina, A. I. Toropov, and K. S. Zhuravlev, *Phys Rev. B* **73**, 035205 (2006).
- ²¹H. Haug and S. Schmitt-Rink, *Prog. Quantum Electron.* **9**, 3 (1984).
- ²²J. H. Collet and T. Amand, *Solid State Commun.* **52**, 53 (1984).
- ²³W. P. Dumke, *Phys. Rev.* **132**, 1998 (1963).
- ²⁴C. H. Lee, *Appl. Phys. Lett.* **30**, 84 (1977).
- ²⁵D. V. Lang and C. H. Henry, *Phys. Rev. Lett.* **35**, 1525 (1975).
- ²⁶K. Ogawa, T. Katsuyama, and H. Nakamura, *Appl. Phys. Lett.* **53**, 1077 (1988).
- ²⁷C. Weisbuch and R. G. Ulbrich, *Phys. Rev. Lett.* **39**, 654 (1977).
- ²⁸F. Jin, T. Itoh, and T. Goto, *J. Phys. Soc. Jpn.* **58**, 2586 (1989).
- ²⁹A. Laubereau, D. V. der Linde, and W. Kaiser, *Opt. Commun.* **7**, 173 (1973).
- ³⁰W. P. Dumke, *Phys. Rev.* **105**, 139 (1957).
- ³¹F. Cadiz, D. Paget, A. C. H. Rowe, L. Martinelli, and S. Arscott, *Appl. Phys. Lett.* **107**, 162101 (2015).
- ³²G. L. Bir, A. G. Aronov, and G. E. Pikus, *JETP* **42**, 705 (1975); *Zh. Eksp. Teor. Fiz.* **69**, 1382 (1975).
- ³³J. H. Jiang and M. W. Wu, *Phys Rev. B* **79**, 125206 (2009).
- ³⁴F. Meier and B. P. Zakharchenya, *Optical Orientation* (Elsevier Science, New York, 1984).
- ³⁵G. Fishman and G. Lampel, *Phys Rev. B* **16**, 820 (1977).
- ³⁶W. Ekardt, K. Losch, and D. Bimberg, *Phys Rev. B* **20**, 3303 (1979).
- ³⁷S. B. Nam, D. C. Reynolds, C. W. Litton, R. J. Almassy, T. C. Collins, and C. M. Wolfe, *Phys. Rev. B* **13**, 761 (1976).
- ³⁸M. Shinada and S. Sugano, *J. Phys. Soc. Jpn.* **21**, 1936 (1966).
- ³⁹M. Z. Maialle, *Phys. Rev. B* **54**, 1967 (1996).
- ⁴⁰B. Urbaszek, X. Marie, and T. Amand, *Rev. Mod. Phys.* **85**, 79 (2013).
- ⁴¹F. Cadiz, D. Paget, A. C. H. Rowe, E. Peytavit, and S. Arscott, *Appl. Phys. Lett.* **106**(9), 092108 (2015).
- ⁴²M. L. Lovejoy, M. R. Melloch, and M. S. Lundstrom, *Appl. Phys. Lett.* **67**, 1101 (1995).
- ⁴³G. W. Fehrenbach, W. Schafer, J. Treusch, and R. G. Ulbrich, *Phys. Rev. Lett.* **49**, 1281 (1982).